Application of Temperature and Pressure Sensitive Paint to an Obliquely Impinging Jet

Jim Crafton*, Nate Lachendro*, Marianne Guille*, and John P. Sullivan†
School of Aeronautics and Astronautics
Purdue University, West Lafayette, IN
Jeffrey D. Jordan‡
Innovative Scientific Solutions Incorporated, Dayton, Ohio

Abstract

Experiments are performed on sonic under-expanded and subsonic jets issuing from a converging nozzle and impinging on a flat plate at oblique incidence. Results are reported on two geometric configurations, jet impingement angles of 10 and 20 degrees at impingement distances of 3.8 and 4.5 jet diameters respectively. The jet velocity was varied from Mach 0.3 to Mach 1.0 while experimental measurements of surface temperature, pressure, and heat transfer coefficient are made using temperature and pressure sensitive paint. Surface measurements are complemented by schlieren flow visualization for the sonic test conditions. In each test configuration the location at which the heat transfer is a maximum is found upstream (in the direction of the nozzle) of the point of maximum pressure recovery and each point of maximum pressure/heat transfer is located upstream of the geometric impingement point (defined as the intersection of the jet axis and the impingement plate). In each case the location of the point of maximum pressure/heat transfer coefficient was found to be a function of impingement angle and impingement distance but independent of Reynolds number. The peak value of heat transfer is about 30% lower than the value predicted at the stagnation point of a normally impinging jet by laminar stagnation theory. The adiabatic wall temperature on the impingement surface is determined experimentally using temperature-sensitive paint.

Introduction

The flow field associated with a subsonic or sonic jet impinging normally on a flat plate has been studied extensively[1 2 3 4 5]. A slight modification to this arrangement is a sonic or subsonic jet impinging obliquely onto a flat plate. This flow field has received comparatively little treatment even though it is encountered in practical arrangements such as, the externally blown flap and exhaust deflectors, as well as situations where geometric constraints require oblique impingement. Of the reports currently available on the subject of obliquely impinging jets none offer a comprehensive data set which includes the distributions of pressure and heat transfer coefficient over the impingement surface. This situation is partially due to the experimental techniques available to previous researchers, the spatial resolution of thermocouples and pressure taps required for a complete survey of the impingement surface is not practical. By applying the technologies of temperature and pressure sensitive paints to the obliquely impinging jet high resolution temperature and pressure distributions on the impingement surface can be acquired. Temperature sensitive paint can also be used for high resolution heat transfer coefficient measurements as well as determination of the adiabatic wall temperature. These experimental techniques along with schlieren flow visualization will be used to analyze the complex flow field of the obliquely impinging jet. The results from the current experiments will be compared to the results reported by previous researchers.

Background

Several studies of the obliquely impinging jet have been conducted. An effort is made to compare the results of the current experiment to the results of previous studies. This required compiling the quantitative and qualitative findings from the previous reports. Unfortunately, most were concerned with only a single surface quantity, pressure or heat/mass transfer.

Perry[6] first studied the heat transfer between an obliquely impinging jet and a flat plate by using an imbedded calorimeter to obtain local heat transfer coefficients. Perry's results lack sufficient spatial resolution due to the fact that the diameter of the calorimeter was equivalent to the diameter of the impinging jet.

Foss[7] made measurements of surface static pressure, velocity, and turbulent intensity in an obliquely impinging axisymmetric jet. The test were

* Research assistant, Member AIAA
† Professor of Aerodynamics, Member AIAA
‡ Analytical Chemist, Member AIAA

conducted at an impingement distance of 4.95 jet diameters, an impingement angle of forty-five degrees, and a jet Mach number of 0.1. Foss reports a that the point of maximum static pressure on the surface coincides with the stagnation point, however, this point is displaced from the geometric impingement location defined by the intersection of the impingement plate and the jet axis. The stagnation point is displaced along the plate in the direction of the nozzle. Foss and Kleis[8] also made a study of an axisymmetric jet impinging obliquely at less than 15 degrees. The displacement of the stagnation point in the direction of the nozzle from the geometric impingement point is also reported in this experiment, however, the point of maximum pressure no longer coincides with the stagnation point.

Sparrow and Lovell[9] used naphthalene sublimation to make mass transfer measurements of low speed jets (Mach number < 0.1) impinging obliquely onto a flat plate. The test conditions included impingement distances of 7 to 15 jet diameters and impingement angles between 90 degrees (normal impingement) and 30 degrees. The results indicate a displacement of the point of maximum mass transfer from the geometric impingement point in the direction of the nozzle. This displacement increased with increasing jet inclination. The maximum and average mass transfer coefficient is reported to decrease by less than 20% as a result of jet inclination.

Goldstein and Franchett[10] made heat transfer measurements of low speed (Mach number < 0.1) obliquely impinging jets using liquid crystals. The test conditions include impingement distances of 4 to 10 jet diameters and impingement angles of 90 degrees to 30 degrees. Once again, the location of maximum heat transfer is displaced from the geometric impingement point in the direction of the nozzle.

A study of heat transfer between a flat plate and a supersonic jet impinging obliquely on it was conducted by Lee[11]. The experimental apparatus employed a series of embedded thermocouples and a transient heat transfer model. Due to the limited number of thermocouples, high spatial resolution was not possible. Results indicate a symmetric distribution of heat transfer in the cross-stream direction. Once again, the point of maximum heat transfer is displaced from the geometric impingement point in the direction of the nozzle.

Lamont and Hunt[12] conducted experiments to study oblique impingement of supersonic jets in the near field. Data collected include surface pressure distributions and shadowgraph pictures. Pressure distributions show that pressure recovery at inclined angles can be much higher than at normal incidence due to multiple shocks between the nozzle and the impingement plate.

Donaldson and Snedeker[13] made an extensive study of the axisymetric jet impinging on several surfaces. Results reported show that at large impingement distances (> 20 jet diameters) the jet profile becomes self similar and the location of maximum pressure recovery becomes a function of impingement angle.

Of the known studies only Reda and Wilder[14] report both surface pressure and shear stress, a quantity related to heat transfer, on an obliquely impinging jet. Their study was primarily concerned with demonstrating the dual implementation of pressure sensitive paint and shear sensitive liquid crystals, therefore, only a single test configuration was considered.

Experiment Apparatus

The experiments will focus on the measurement of surface properties, specifically temperature, pressure, and heat transfer coefficient on the impingement surface. The goal is to locate the point of maximum pressure recovery, and the point of maximum heat transfer relative to the geometric impingement point. In addition to the surface measurements, schlieren flow visualization will be used to study the shock structure of the flow in the sonic case. The flow visualization will be correlated to the surface measurements. The experimental apparatus and test facility are described in the following sections.

Test Facility

The jet/impingement plate configuration is shown in figure 1. The jet consists of a five-inch diameter by twelve-inch long settling chamber with a one-half inch radial inlet to a five millimeter diameter nozzle with a fifteen degree convergence angle. The settling chamber is instrumented with a J type thermocouple to monitor the jet total temperature. The total pressure is set using a regulator and monitored using a 0.2 psi resolution Heise gauge. Compressed air is supplied to the nozzle from the Purdue University ASL PAC air system. The impingement plate is an eight-inch high by twenty-inch long by one-half inch thick aluminum plate. The geometric impingement distance (H/D) and the impingement angle (θ) can be varied independently to produce multiple impingement configurations. Impingement angles of 20 degrees and 10 degrees (90 degrees corresponds to normal impingement) will be tested. The geometric

impingement distance (H) will be set near four jet diameters. The coordinate system which will be used to present the results is also shown in figure 1. The origin of the coordinate system (S,Y) will coincide with the geometric impingement point (defined as the intersection of the impingement surface and the jet axis). The S coordinate extends along the surface of the impingement plate in the stream-wise direction. The Y coordinate extends along the surface of the impingement plate in the cross stream direction.

Temperature Sensitive Paint

High resolution, non-intrusive measurements of temperature and heat transfer using temperature sensitive paint have been demonstrated by Liu[1] [19] and Campbell[15] . A typical TSP consists of the luminescent molecule and an oxygen impermeable binder. The basis of the temperature sensitive paint method is the sensitivity of the luminescent molecules to their thermal environment. The luminescent molecule is placed in an excited state by absorption of a photon. The excited molecule deactivates through the emission of a photon. A rise in temperature of the luminescent molecule will increase the probability that the molecule will return to the ground state by a radiationless process. This process is known as thermal quenching and is the basis of temperature sensitive paint. The temperature of the painted surface can be measured by detecting the fluorescence intensity I(T) of the luminescent paint.

The luminescent intensity of the temperature sensitive paint at a given point is not only a function of temperature. For practical applications of TSP spatial variations in illumination, paint concentration, paint layer thickness, and camera sensitivity will result in a variation in the detected luminescent intensity from the test surface. These spatial variations are eliminated by ratioing the luminescent intensity of the paint at the unknown test condition (I_T) with the luminescent intensity of the paint at a known reference condition (I_{ref}, T_{ref}).

Temperature Sensitive Paint Calibration

A mixture of Tris(2,2'-bipyridyl)ruthenium(II) chloride hexahydrate (Ru(bpy)) and model airplane dope was the temperature paint used in these experiments. The TSP was calibrated over a range of temperature from 15 [C] to 85 [C]. The data was fit to a second order polynomial. The resulting calibration of intensity ratio as a function of temperature ratio is given in equation 1. The calibration data and polynomial curve fit are shown in figure 2.

$$\frac{I(T)}{I(T_{ref})} = 1.25 - 0.36\left(\frac{T}{T_{ref}}\right) + 0.10\left(\frac{T}{T_{ref}}\right)^2 \quad (1)$$

Pressure Sensitive Paint

Traditional measurement techniques for acquiring surface pressure distributions on models have utilized embedded arrays of pressure taps. This requires much construction and setup time while producing data with limited spatial resolution. An alternative approach is to use pressure (oxygen) sensitive paint to measure surface pressure. Pressure measurements using pressure sensitive paints have been demonstrated in several challenging flow fields such as an operating compressor blade[16] and an aircraft wing[17] in flight. The advantages of pressure sensitive paint include non-intrusive pressure measurements and high spatial resolution when compared to conventional measurement techniques.

A typical pressure sensitive paint is comprised of two main parts, as shown in figure 3, an oxygen sensitive fluorescent molecule, and an oxygen permeable binder. The pressure sensitive paint method is based on the sensitivity of certain luminescent molecules to the presence of oxygen. When a luminescent molecule absorbs a photon, it is excited to an upper singlet energy state. The molecule then typically recovers to the ground state by the emission of a photon of a longer wavelength. In some materials oxygen can interact with the molecule so that the transition to the ground state is radiationless, this process is known as oxygen quenching. The rate at which these two processes compete is dependent on the partial pressure of oxygen present, with a higher oxygen pressure quenching the molecule more, thus giving off a lower intensity of light.

Unfortunately, pressure sensitive paints are also sensitive to temperature. A rise in temperature will increase the probability that the molecule will transition back to the ground state by a radiationless process. This process is known as thermal quenching. A second source of temperature sensitivity occurs when the binder for pressure sensitive luminescent molecule has a permeability that is a function of temperature. This is often the case for the polymer based binders used for pressure sensitive paint. Temperature sensitivity can lead to many problems in converting the intensity distributions to pressure if not taken into account. Effective implementation of a pressure sensitive paint, therefore, requires that temperature effects be characterized and corrected, or the paint be used in an isothermal environment. This

problem is especially apparent in flows with small pressure (1 [psi]) changes in the presence of a moderate (1 [K]) temperature gradient. Here the temperature dependent intensity changes would be on the order of the pressure dependent intensity changes. Once again, non-uniform illumination, paint thickness and concentration, and camera sensitivity are eliminated by a ratioing process involving the luminescent intensity at a known condition (I_{ref}, P_{ref}).

Pressure Sensitive Paint Calibration

A mixture of bathophen ruthenium chloride (Ru(ph2-phen)) in RTV was utilized as a pressure sensitive paint for the oblique jet impingement experiments. The PSP was calibrated over a range of temperatures from 15 [C] to 40 [C] and a range of pressures from 1 [psia] to 50 [psia]. The reference conditions were chosen as 14.56 [psia] and 25 [C]. Analysis of the calibration data yielded a power law equation for intensity ratio as a function of temperature and pressure. The calibration data, along with the power law correlation is shown in figure 4. The calibration equation is given as equation 2. The PSP exhibited a pressure sensitivity of 3.1% per [psi] and a temperature sensitivity of -1.3% per [C].

$$\frac{I_{ref}}{I} = \left\{ 4.0\, Ln\left(\frac{T}{T_{ref}}\right) + 1.0 \right\} \left(\frac{P}{P_{ref}}\right)^{0.45} \qquad (2)$$

The apparatus used to calibrate the PSP is not capable of withstanding the full pressure range (up to 50 [psia]) which could be encountered in this experiment. However, as stated previously, the intensity of the PSP is a function only of the partial pressure of oxygen. This fact was exploited in the calibration process in a manner following Erausquin[18]. Two sets of calibration data were acquired at each temperature, one using air as the working gas, the other using oxygen. The pressure of the calibration data acquired using oxygen as the working gas was converted to an equivalent ambient air pressure with that partial pressure of oxygen. This allowed the range of the calibration to be extended beyond the range of pressures encountered in the experiment.

PSP / TSP Data Acquisition and Reduction

The CCD camera system for the luminescent paints is the most commonly used in aerodynamic testing. A schematic of this system is shown in figure 5. The luminescent paint (TSP or PSP) is coated on the surface of the model and the paint is excited to luminesce by light from a blue LED array (λ= 460 nm). The luminescent intensity from the paint on the model surface, which is temperature or pressure sensitive, is optically long pass filtered (570 nm) to eliminate the excitation light and then captured by a 16 bit CCD camera (Photmetrics). Both a flow-on image and a reference image are obtained. The ratio between the flow on image and reference image is then converted to temperature or pressure using the previously determined calibration relations.

Heat Transfer Measurements

Heat transfer measurements require a surface heat flux. In the current experiment this heat flux must be generated by heating/cooling of the jet air source, or global heating/cooling of the impingement surface. The second option, heating of the impingement surface, was selected. The experimental arrangement of the heat transfer measurement plate is shown in figure 6. The heat transfer analysis, following Liu[19], assumes one-dimensional steady state conduction. A one-half inch thick aluminum plate is covered on one side with a 0.28 millimeter thick sheet of mylar. A TSP, Ru(bpy) in model airplane dope, is applied to the surface of the mylar. The aluminum plate is heated to a uniform temperature, T_w , which results an isothermal boundary on the back surface of the insulating mylar layer. The front (TSP side) surface of the plate is illuminated with 460 nm excitation from a blue LED array and exposed to the jet flow. The intensity distribution of the TSP surface is recorded using a CCD camera, this intensity distribution is then converted to a surface temperature (T_s) distribution as discussed previously. The local heat flux can be determined at this point as:

$$q = k\frac{\left(T_w - T_s\right)}{L} \qquad (3)$$

Where L is the thickness of the mylar and k is the thermal conductivity of the mylar. The local heat flux is related to the local convection heat transfer coefficient, h, through:

$$q = h\left(T_s - T_{aw}\right) \qquad (4)$$

Here T_{aw}, the adiabatic wall temperature is used to complete the heat transfer calculation in equation 4.

The adiabatic wall temperature is defined as, the temperature at the surface of the wall when the heat flux is zero. The current experimental setup, does not lend itself to enforcing the adiabatic boundary condition necessary to make this measurement directly, however, an indirect method is suggested by Lee[20]. In the current experiment, the adiabatic wall temperature and the heat transfer coefficient are constants. However, the current experimental setup allows the surface temperature T_s to be measured

directly while the heat flux is controlled by varying T_w. The adiabatic wall temperature is found by making measurements of T_s at each of several values of q, and thus T_w. A plot of T_s versus q reveals a linear relationship between T_s and q as suggested by equation 3. The adiabatic wall temperature is found by fitting a least squares line through the data points and extrapolating the line to the point where q is equal to zero. This process is demonstrated at the geometric impingement point for two test configurations in figure 7. The extrapolation process is repeated at each point on the surface of the impingement plate yielding a 2-dimensional adiabatic wall temperature distribution for each test condition.

Schlieren

The near field of the sonic jet contains several shock waves and expansion fans. As the impingement plate enters the near field of the jet these waves will interact with the impingement plate. The resulting temperature and pressure distributions on the impingement surface are studied using temperature and pressure sensitive paints. The surface measurements are complimented with schlieren flow visualization.

The single pass schlieren system used is shown in figure 8, the standard Z arrangement is employed. The system consists of a General Radio Company model 1538-A Strobotac light source, a pair of 6 inch diameter concave mirrors, a knife edge, and a Photometrics 16 bit CCD camera. A pair of 6 inch by 6 inch flat front surface mirrors are used to orient the schlieren in the vertical plane, parallel to the impingement plate and normal to the jet axis. With this arrangement a single surface quantity (temperature or pressure) and a schlieren image are acquired at each test condition.

The schlieren images will indicate the structure of the jet flow above the impingement surface along a single line. The line selected is along the axis of symmetry of the jet in the stream-wise direction. The surface measurements along this line are to be correlated with the corresponding schlieren image, however, this requires some form of image registration. This issue is resolved by determining the relative magnification of the two images and locating a common point in the two images.

Data Acquisition System

During the course of these experiments it has been observed that the shock wave/expansion fan structure of the obliquely impinging jet flow field is extremely sensitive to the test conditions. It was determined that the schlieren images must be taken simultaneously with the TSP/PSP images to be of significant value. The physical setup to accomplish this task required a PSP/TSP system (oriented normal to the impingement plate) to be combined with a schlieren system (oriented perpendicular to the impingement plate) and a PC based data acquisition system which controls two cameras. This type of two camera data acquisition system is commonly employed in the field of image based velocimetry with techniques such as Planer Doppler Velocimetry[21] (PDV) and Particle Image Velocimetry (PIV). Schlieren and PSP/TSP images were acquired simultaneously and combined into a single file for storage using a single PC and two 16 bit Photometrics CCD cameras.

Results

The results of the pressure and heat transfer measurements on the impingement surface of the obliquely impinging jet at 10 and 20 degrees were collected and compared to the results presented in previous studies. The complete data set covers a wide range of Mach numbers, impingement angles, impingement distances, and nozzle geometries.

Pressure Measurements

The temperature sensitivity of the pressure sensitive paint was an issue of major concern in the current experiment. A 1 [C] change in the temperature of the ruthenium based pressure paint results in a 1.3% change in the intensity of the paint. This would appear as a 0.3 [psi] change in pressure. Much care was taken to insure that the stagnation temperature of the jet was equal to the ambient temperature, however this does not insure that the surface of the impingement plate is isothermal and equal to the ambient temperature.

As the flow expands through the nozzle static pressure (potential energy) is converted, isentropically, to kinetic energy (velocity). Near the impingement plate the flow decelerates from its local free stream velocity through a viscous boundary layer and stagnates on the surface. In this case the conversion of the kinetic energy to static pressure is not isentropic due to the viscous effects in the boundary layer. The losses associated with this non-isentropic process are quantified by the recovery factor, r, which is a function of Prandtl number. The relations for recovery factor given by White[22] for laminar and turbulent boundary layers are, respectively:

$$r = \sqrt{\mathrm{Pr}} \tag{5}$$

$$r = \sqrt[3]{\mathrm{Pr}} \tag{6}$$

The ramifications of the recovery factor on the current experiment are outlined in figure 9. On the surface of the PSP the flow stagnates resulting in a local static temperature, the adiabatic wall temperature. An analysis based on one-dimensional steady state conduction results in the following relationship between the temperatures of the wall, the PSP, and the flow.

$$T_s - T_w = \frac{(T_w - T_{aw})\frac{hL}{k}}{\left(1 - \frac{hL}{k}\right)} \qquad (7)$$

The difference between T_s and T_w must be minimized to eliminate temperature effects on the pressure sensitive paint measurement. Of the variables in equation 7, only L is easily modified. Examination of equation 7 reveals that a as L approaches zero T_s approaches T_w. This suggest a solution consisting of thin paint layer on a wall with a high thermal conductivity. Generally, a white base, usually mylar or paint, is applied to the model surface to be tested and the PSP is coated onto this base. The configuration used in these test consists of a thin layer of PSP painted directly on an aluminum plate. The high thermal conductivity of aluminum should result in a constant value of T_w while the thin paint layer will minimize any deviation between T_s and T_w over the impingement surface.

This theory was tested by applying a thin layer of TSP with a thermal conductivity and thickness similar to that of the PSP to be tested onto the aluminum impingement plate. The temperature distribution over the impingement surface for a sonic jet is shown in figure 10. The impingement surface temperature varies by less than 0.5 [C] from the region outside of the influence of the jet to any location inside the region of influence of the jet. This would result in an error in the PSP measurement of about 0.1 [psi]. The corresponding pressure distribution found using PSP is shown in figure 11. Here the pressure varies by more than 8 [psi] suggesting a temperature induced error of less than 3% of full range due to temperature effects.

The stream-wise pressure distribution for each test condition at impingement angles of 10 degrees and 20 degrees is plotted in figure 12. The subsonic pressure distributions show a single peak pressure, the stagnation point. This peak pressure location does not deviate significantly with Reynolds number but does change with impingement angle. The first pressure peak in the sonic jet pressure distributions coincides with the single peak from the subsonic distributions and will be treated as the stagnation point. In all cases this peak location is found upstream (in the direction of the nozzle) of the geometric impingement point (defined as the intersection of the jet axis and impingement plate). A correlation of this peak pressure location is suggested by Sparrow[9] and Lovell, this correlation is represented in figure 13. The distance between the geometric impingement point and the point of maximum pressure recovery, ΔS, is non-dimensionalized by the impingement distance, H, and plotted versus impingement angle θ. The data points at 10 and 20 degrees contain data over a wide range of Reynolds numbers at an impingement distance of 3.8 and 4.5 jet diameters respectively. The data of Doneldson and Snedeker covers a range from 90 degrees (normal impingement) to 30 degrees at 1.96 to 39.1 jet diameters. Figure 13 suggests that in the far field, $\Delta S/H$ becomes only a function of impingement angle. This could be a result of a developing jet profile which is becoming self similar. In the near field, specifically inside the jet potential core, $\Delta S/H$ is a function of impingement angle and impingement distance. There is some variation of $\Delta S/H$ at a given impingement angle and impingement distance in the near field with jet velocity. This variation, however, is small compared to the effects of impingement angle and distance.

As previously mentioned the pressure distributions for each of the sonic jets contains several peaks and valleys. Some insight into the surface pressure distribution can be gained using schlieren flow visualization. A composite image of the streamwise pressure distribution and schlieren flow visualization in the plane of this pressure distribution for a sonic jet impinging at 10 degrees is shown in figure 14. The location of the intersection of the shock waves with the surface corresponds with the pressure on the impingement surface.

Heat Transfer Measurements

The utility of the current TSP based heat transfer measurement technique is demonstrated in the 2-dimensional heat transfer distribution of a sonic jet shown in figure 15. The high spatial resolution of the image based technique combined with the wide dynamic range of the temperature sensor allows measurements of the heat transfer coefficient and adiabatic wall temperature over the wide range of velocities encountered in this experiment. Images, similar to figure 15, were acquired for each test case and the stream-wise heat transfer distribution for each pressure ratio at an impingement angle of 10 degrees and 20 degrees is plotted in figure 16. Each heat

transfer distribution exhibits a similar structure, a sharp rise downstream of the nozzle to a single peak in the heat transfer distribution followed by a reduction in the heat transfer downstream. Once again, this peak heat transfer coefficient location is located upstream of the geometric impingement location, does not vary significantly with Reynolds number, but does change with impingement angle. The peak heat transfer location is correlated, once again, following Sparrow and Lovell in figure 17. The distance between the geometric impingement point and the point of maximum heat transfer, ΔS, is non-dimensionalized by the impingement distance, H, and plotted versus impingement angle θ. This figure contains data over a wide range of Reynolds numbers, impingement distances, and includes variations in nozzle geometry. This data shows a trend similar to that of the pressure data in figure 13 and therefore suggest some similar conclusions. In the far field ($H/D > 6$) $\Delta S/H$ is only a function of impingement angle. Once again, in the near field $\Delta S/H$ becomes a function of impingement angle and impingement distance. The small variations of $\Delta S/H$ with Reynolds number in the near field are still evident. Note that the heat transfer data of Goldstein and mass transfer data of Sparrow are limited to Mach numbers less than 0.1 while the data from the current experiment ranges from Mach 0.3 to sonic.

Correlation of Maximum Heat Transfer

Goldstein reports a reduction in the peak value of heat transfer as the jet impingement angle is reduced from 90 degrees (normal impingement). The peak value of heat transfer in the current experiment is compared to the results of Goldstien and to a theoretical correlation of laminar stagnation point heat transfer in figure 18. For the purposes of the comparison Nusselt number was plotted versus Reynolds number for several impingement angles. The Reynolds numbers for the current experiment varies from 35,000 to 130,000 while the range covered by the data of Goldstein is only 10,000 to 30,000. The reduction in Nusselt number with decreasing impingement angle is evident in the data reported by Goldstein and the data from the current experiment falls along a line near the 30 degree impingement data of Goldstein with the exception of the data at the highest Reynolds number. It is noted that the jet Reynolds number corresponds to a moderately under-expanded condition while all other data is subsonic or slightly under-expanded.

Location of Maximum Heat Transfer Relative to Maximum Pressure Recovery

With the exception of Reda and Wilder previous experiments have measured a single surface quantity. The single data point presented by Reda and Wilder indicates that the location of peak shear stress (a quantity related to heat transfer) does not coincide with the location of maximum pressure recovery. This is consistent with the a result reported by Foss[8] and Klies (Foss and Klies measured surface pressure and velocity, heat transfer was calculated from these quantities) for a jet impinging at 15 degrees. The deviation of the location of peak heat transfer and the maximum pressure recovery from the geometric impingement point over impingement distance for the current data are plotted in figure 19. Figure 19 appears to support the conclusion that the location of the point of peak heat transfer does not coincide with the point of maximum pressure recovery, however, inspection of the data in figure 19 indicates that this conclusion is a function of the jet Reynolds number. As the jet Reynolds number is increased the distance between the point of maximum pressure recovery and peak heat transfer decreases.

Conclusions

The temperature and pressure sensitive paint techniques were used to make non-intrusive quantitative measurements of the pressure, connective heat transfer coefficient, and adiabatic wall temperature distributions on the surface of a flat plate with a jet impinging obliquely onto it at 10 and 20 degrees. The temperature sensitivity of the PSP was minimized by applying a thin layer of the PSP directly onto an aluminum plate thus enforcing an isothermal wall boundary condition to the pressure sensitive paint. This isothermal condition was verified experimentally by making temperature measurements on the impingement surface using temperature sensitive paint. At each impingement angle the location at which the heat transfer is a maximum is found upstream (in the direction of the nozzle) of the point of maximum pressure recovery. Each point of maximum pressure/heat transfer is located upstream of the geometric impingement point (defined as the intersection of the jet axis and the impingement plate) as in previous studies. In each case the location of the point of maximum pressure/heat transfer coefficient was found to be independent of Reynolds number. The maximum value of heat transfer coefficient was compared to experimental data from Goldstein and to a theoretical correlation based on laminar stagnation theory. The data from the current experiment is

consistent with the experimental results of Goldstein which suggest a reduction in the maximum value of heat transfer coefficient as the impingement angle is decreased from 90 degrees.

Future Work

Future PSP measurements could be made using an aluminum plate with a hydrothermally processed film coating. This new PSP film coating technology, currently under development at Purdue University, results in an extremely thin, uniform layer of a ceramic/polymer film which is a suitable environment for luminescent PSP molecules. The high thermal conductivity of the aluminum combined with the thin PSP layer will result in pressure measurements with the smallest possible temperature effect. Velocity measurements, using point or planer laser velocimetry, could be made to reveal the stagnation point of the flow. Velocity field measurements would also be useful in the analysis of the adiabatic wall temperature for heat transfer measurements.

Acknowledgements

The authors would like to acknowledge Gary Dale for the loan of the blue LED array used in this experiment and William Weaver for developing the software for the PC based 2 camera data acquisition system. We would also like to thank Tianshu Liu for the useful discussions concerning the fluid dynamics and heat transfer considerations associated with this experiment.

References

[1] T. Liu and J. P. Sullivan, "Heat transfer and flow structures in an excited circular impinging jet", Int. J. Heat Mass Transfer, 39, 3695-3706 (1996)

[2] M. S. El-Genk, L. Huang and Z. Guo, "Heat Transfer between a Square Flat Plate and a Perpendicularly Impinging Circular Air Jet", HTD, Enhanced Heat Transfer, 202, 33-38 (1992)

[3] R. Viskanta, "Heat Transfer to Impinging Isothermal Gas and Flame Jets", Experimental Thermal and Fluid Science, 6, 111-134 (1993)

[4] C. D. Donladson, R. S. Snedeker and D. P. Margolis, "A study of free jet impingment. Part 2. Free jet turbulent structure and impingment heat transfer", J. Fluid Mech., 45, 477-512 (1971)

[5] I. B. Ozdemir and J. H. Whitelaw, "Impingement of an axisymmetric jet on unheated and heated flat plates", J. Fluid Mech., 240, 503-532 (1992)

[6] Perry, K. P., "Heat Transfer by Convection from a Hot Gas Jet to a Plane Surface.", Procedings of the Institution of Mechanical Engineers, vol. 168, pp. 775-780, (1954)

[7] Foss, J. F., "Measurements in a Large-Angle Oblique Jet Impingement Flow", AIAA Journal, vol. 17, num. 8, pp. 801-802, (1979)

[8] Foss, J. F. and Kleis, S. J., "Mean Flow Characteristics for the Oblique Impingement of an Axisymmetric Jet," AIAA Journal, vol. 14, pp705, June (1976)

[9] Sparrow, E. M. and Lovell, B. J., "Heat Transfer Characteristics of an Obliquely Impinging Circular Jet", ASME Journal of Heat Transfer, vol. 102, pp202-209, (1980)

[10] Goldstein, R. J. and Franchett, M. E., "Heat Transfer From a Flat Surface to an Oblique Impinging Jet", ASME Journal of Heat Transfer, vol. 110, pp. 84-90, (1988)

[11] Lee, C., Chung, M. K., Lim, K. B., and Kang, Y. S., "Measurements of Heat transfer From a Supersonic Impinging Jet Onto an Inclined Flat Plate at 45 deg.", ASME Journal of Heat Transfer, vol. 113, pp. 769-772, (1991)

[12] Lamont, P. J., and Hunt, B. L., "The impingement of underexpanded, axisymmetric jets on perpendicular and inclined flat plates", Journal of Fluid Mechanics, vol. 100, num. 3, pp. 471-511, (1980)

[13] C. D. Donladson, R. S. Snedeker and D. P. Margolis, "A study of free jet impingement. Part 1. Free jet turbulent structure and impingement heat transfer", J. Fluid Mech., 45, 281-512 (1971)

[14] Reda, D. C., Wilder, M. C., Mehta, R. D., and Zilliac, G. “Measurements of Continuous Pressure and Shear Distributions Using Coating and Imaging Techniques”, AIAA Journal, vol. 36, pp. 895-899, (1998)

[15] Campbell, B. T., Crafton, J., Witte, G., Sullivan, J. P., “Laser Spot Heating/Temperature Sensitive Paint Heat Transfer Measurement System”, AIAA-98-2501 (1998)

[16] Liu, T. S., Torgerson, S. D., Sullivan, J. P., “Rotor Blade Pressure Measurements in a High Speed Axial Compressor using Pressure and Temperature Sensitive Paints”, AIAA-97-0162 (1997)

[17] Lachendro, N., Crafton, J., Guille, M., Sullivan, J. P., “In Flight Pressure Measurements of a Transonic Wing Using A Pressure Sensitive Paint Based Laser Scanning System”, PSP Workshop, Seattle WA, (1998)

[18] Erausquin, R., Cunningham, C., Sullivan, J. P., "Cryogenic Pressure Sensitive Fluorescent Paint Systems", AIAA-98-088, (1998)

[19] Liu, T., Campbell, B. T., Sullivan, J. P., “Fluorescent paint for Measurement of Heat Transfer

in Shock-turbulent Boundary layer Interaction", Experimental Thermal and Fluid Science, vol. 10, pp. 101-112, (1995)
[20] Lee, Y., Settles, G. S., and Horstman, C. C., "Heat Transfer Measurements and Computations of Swept-Shock-Wave/Boundary-layer Interactions", AIAA Journal, vol. 32, pp. 726-734, (1994).
[21] Beutner, T. J., Williams, G. W., Baust, H. D., Elliott, G. S., Crafton, J., Carter, C. D., "Characterization and Applications of Doppler Global Velocimetry", AIAA 99-0266, (1999)
[22] White, F. M., "Viscous Fluid Flow", 2ond ed., McGraw-Hill, (1991)

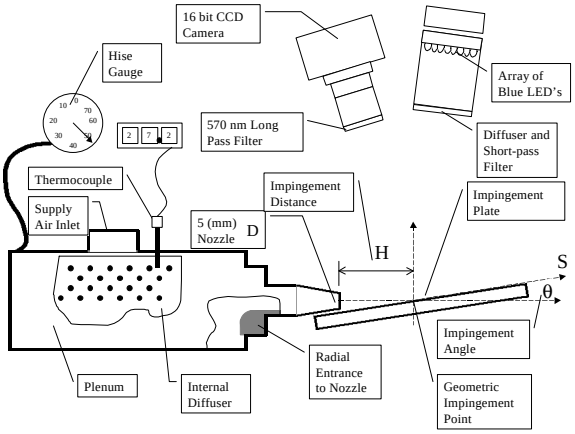

Figure 1 Schematic of the obliquely impinging jet test facility.

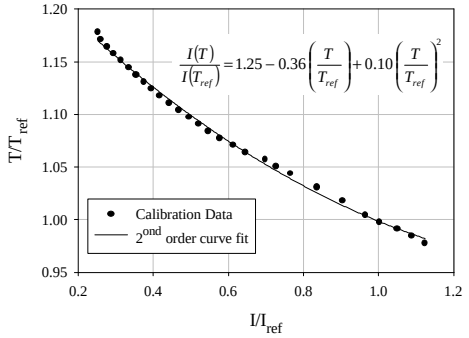

Figure 2 Calibration of the Temperature Sensitive Paint, Tris(2,2'-bipyridyl)ruthenium(II) chloride hexahydrate in dope.

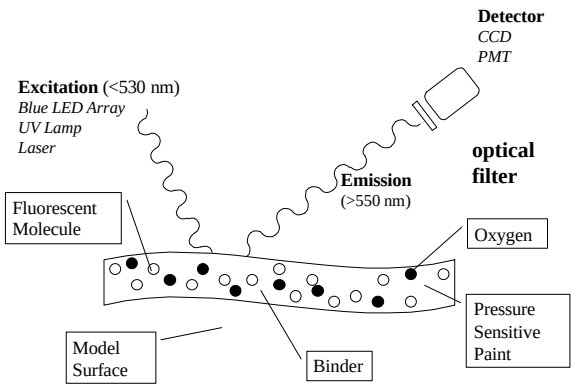

Figure 3 Components and basic operation of pressure sensitive paint measurement system.

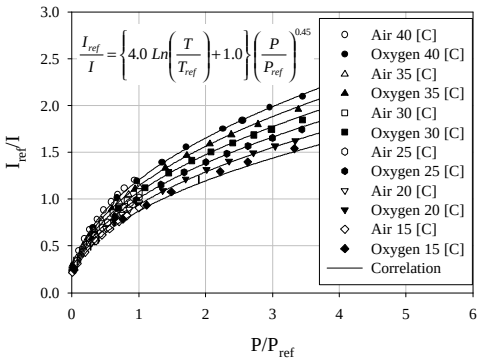

Figure 4 Calibration of Pressure Sensitive Paint bathophen ruthenium chloride (Ru(ph2-phen)) in RTV at several temperatures.

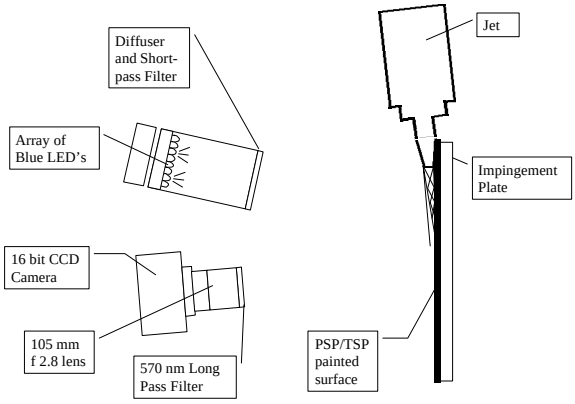

Figure 5 CCD camera based Temperature and Pressure sensitive paint data acquisition system.

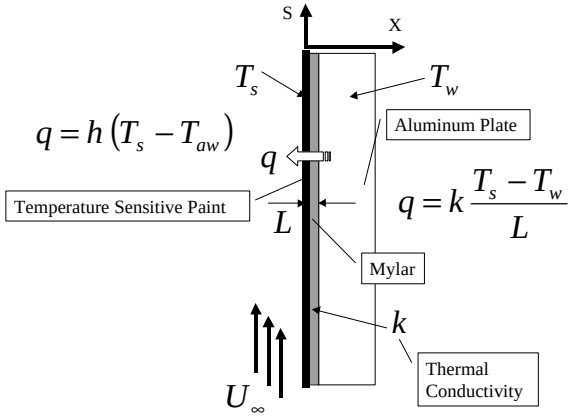

Figure 6 Experimental set up for heat transfer measurement.

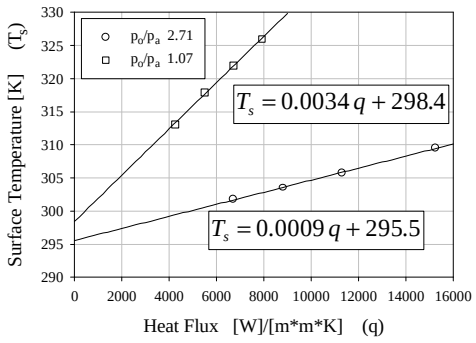

Figure 7 Plot of wall heat flux, (q) versus wall temperature, (T_s) at the geometric impingement point for two jet velocities. The jet stagnation temperature is 299.5 [K] in each case.

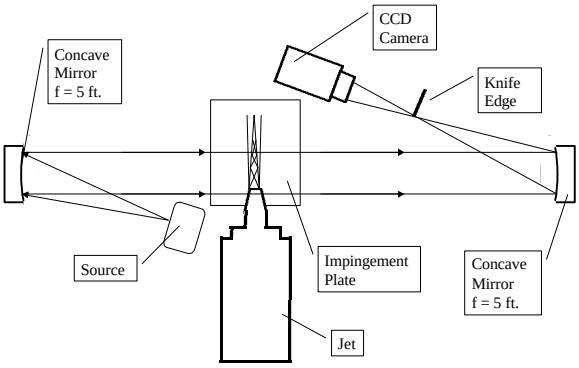

Figure 8 Single pass schlieren system.

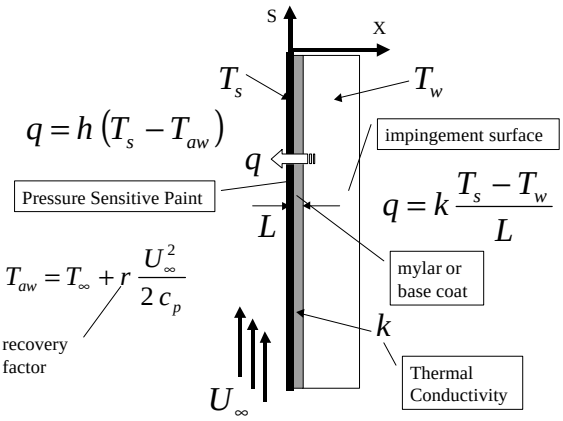

Figure 9 Design considerations for minimizing temperature effects on a PSP measurement due to the recovery factor.

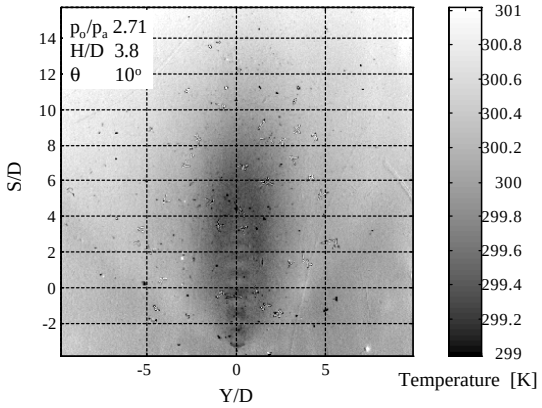

Figure 10 Temperature distibution on the impingement surface of a sonic jet.

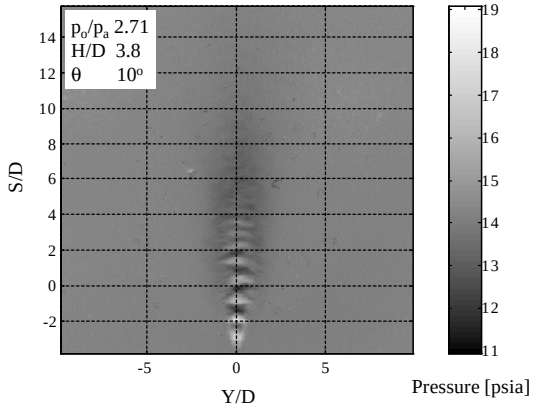

Figure 11 Pressure distribution on the impingement surface of a sonic jet.

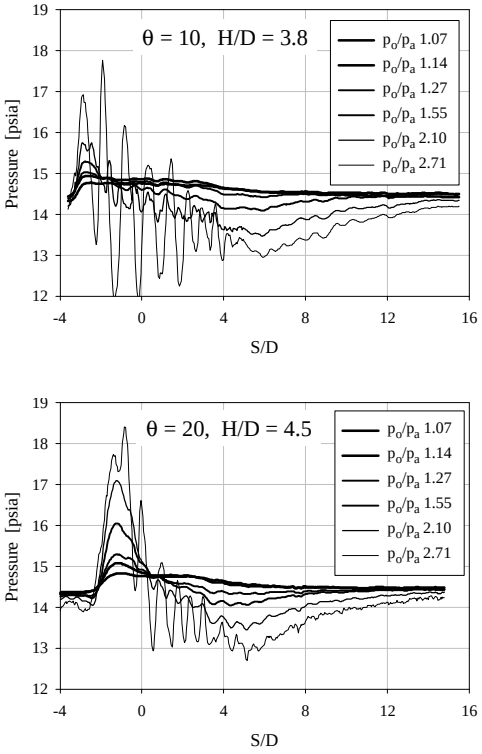

Figure 12 Stream-wise pressure distribution on the axis of symmetry.

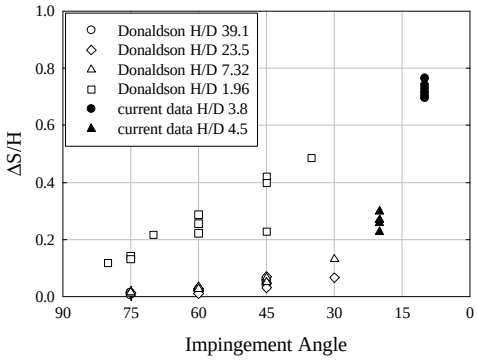

Figure 13 Displacement of the point of maximum pressure recovery from the geometric impingement point over impingement distance versus impingement angle.

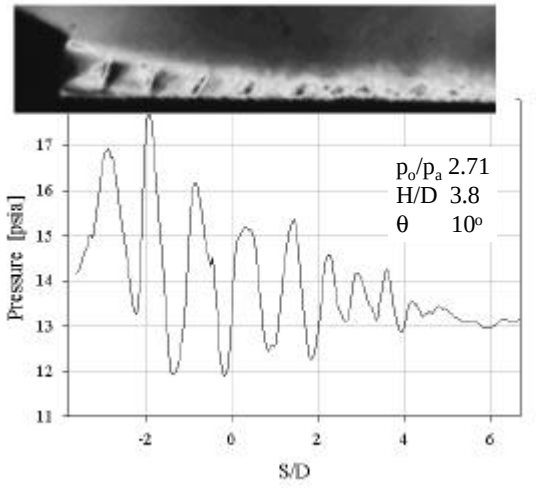

Figure 14 Composite image of the streamwise pressure distribution with schlieren flow visualization for a sonic jet.

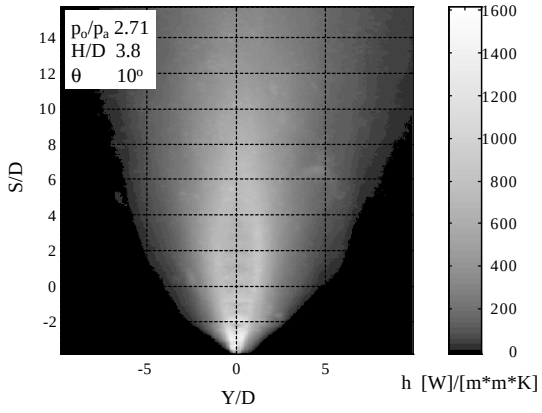

Figure 15 Heat transfer distribution on the impingement surface of a sonic jet.

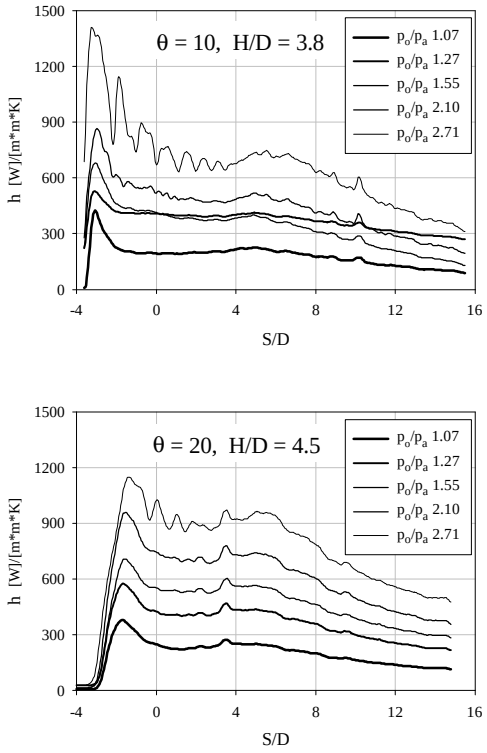

Figure 16 Stream-wise heat transfer coefficient distribution at the axis of symmetry.

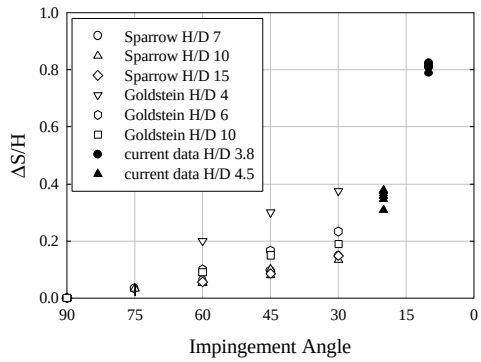

Figure 17 Displacement of the point of maximum heat transfer from the geometric impingement point over impingement distance versus impingement angle.

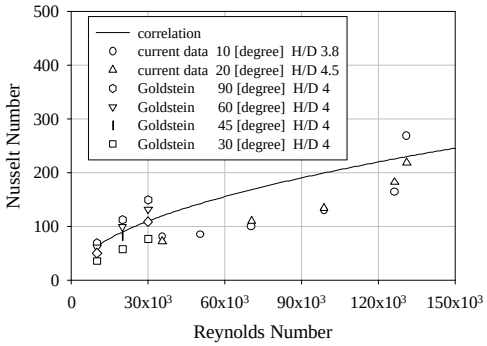

Figure 18 Maximum Nusselt number versus jet Reynolds number. Plot contains the data from the current experiment, data from Goldstein, and a correlation based on laminar stagnation theory.

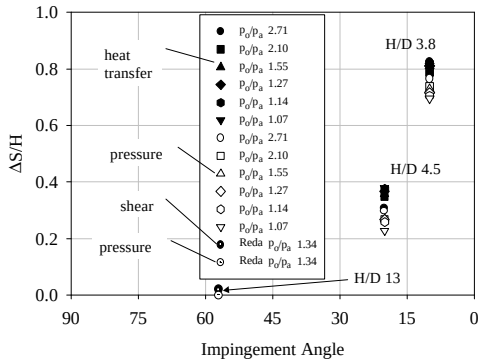

Figure 19 Deviation of the location of peak heat transfer and maximum pressure recovery from the geometric impingement point divided by impingement distance versus impingement angle.